Pergamon

Journal of Structural Geology, Vol. 18, No. 1, pp. 17 to 25, 1996

0191-8141/96 $15.00+0.00

0191-8141(95)00074-7

The role of intragranular fracturing on grain size reduction in feldspar during mylonitization

KATSUYOSHI MICHIBAYASHI*

Department of Earth Science, James Cook University, Townsville, QLD 4811, Australia

(*Received* 8 *February* 1994; *accepted in revised form* 26 *June* 1995)

Abstract—Measurements of the size, shape and orientation of K-feldspar and plagioclase grains within a granitic mylonite in the Kashio shear zone, central Honshu, Japan, revealed that grain size was the most effective parameter controlling development of intragranular fracturing during mylonitization. Intragranular fractures are dominantly located near the centre of each grain and form preferentially along the (001) cleavage. The grain size distribution of both feldspars is log-normal with an average of 760 μm. The proportion of fractured grains expands dramatically to 100% as the grain size increases, whereas few feldspar grains smaller than 300 μm have been fractured during the mylonitization, indicating that the fractures have preferentially developed in coarser grains. Furthermore, the shape and shape-preferred orientation of feldspar grains also affects the development of fractures. The proportion of fractured grains not only increases up to 20% towards the extension direction, but also rises slightly as the aspect ratio of feldspar grains increases. It is, therefore, suggested that feldspar grains lying perpendicular to the extension direction may resist fracturing regardless of grain size, unless their shape-preferred orientations became sub-parallel to the extension direction due to rotation or modification of their grain shapes during mylonitization. The development of intragranular fractures could be statistically explained in terms of a fibre-loading model, although individual fractures may result from various fracture mechanisms.

INTRODUCTION

During the development of mylonitic microstructure in polymineralic rocks, some minerals (e.g. quartz) may deform plastically while others (e.g. feldspar) may behave in a brittle manner, resulting in the formation of porphyroclasts. The shape and distribution of such porphyroclasts can provide kinematic information on shear sense (e.g. Berthé *et al.* 1979, Simpson & Schmid 1983, Passchier & Simpson 1986, Takagi & Ito 1988, Hippertt 1993) and non-coaxiality (e.g. Passchier 1987, Hanmer 1990, Masuda *et al.* 1995) in many shear zones.

In low- to medium-grade mylonitic rocks, porphyroclasts are often fractured into segments within a plastically deformed matrix (intragranular fractures; see Fitz-Gerald & Stunitz 1993 for review), where fractures are commonly tensile (O'Hara 1990, Michibayashi & Masuda 1993, Bailey *et al.* 1994). Tensile fracturing is theoretically considered to occur when the tensile stress exceeds the tensile fracture strength of the grain during stress transfer (i.e. the fibre-loading model; Cox 1952, Lloyd *et al.* 1982, Masuda *et al.* 1989, Ji & Zhao 1993). However, these theoretical models are essentially for coaxial deformation, whereas the kinematic frame during mylonitization is generally non-coaxial (Passchier 1987, Hanmer 1990, Masuda *et al.* 1995). Lack of data from natural mylonites also makes it difficult to expand the theoretical models into general non-coaxial deformations (Ji & Zhao 1993).

Intragranular fractures in mylonite are associated with other deformation mechanisms such as intracrystalline plasticity and diffusive mass transfer (Lloyd & Knipe 1992, Bailey *et al.* 1994), resulting in a range of different microstructures. The process of fracturing tends to be obscured because fracture walls may be subsequently recrystallized or chemically replaced by other minerals during progressive shearing (Fitzgerald & Stunitz 1993). Alternatively, sub-critical fracturing may also occur during mylonitization (Atkinson 1982, 1984, White & White 1983, Hanmer 1981, Prior 1993).

This paper presents a series of data collected in feldspar porphyroclasts of a granitic mylonite from the Kashio shear zone, Japan. In this mylonite, intragranular fractures in feldspar are well preserved, and neither chemical replacement nor recrystallization occurred along the fracture walls. These features made it possible to study the development of intragranular fracturing in this natural shear zone.

GEOLOGICAL SETTING

The granitic mylonite described here was sampled in the Kashio shear zone within the Ryoke metamorphic belt in the Chubu district, Japan (Hara *et al.* 1977, 1980, Takagi 1986, Michibayashi & Masuda 1993, Michibayashi 1993, Ohtomo 1993, Yamamoto 1994). This shear zone developed within the southeastern margin of the Ryoke Cretaceous plutonic complex that intrudes the Ryoke high temperature/low pressure metamorphic rocks (Ryoke Research Group 1972, Kano 1978) along the Median Tectonic Line.

The sample in this study was collected from

*Present address: Institute of Geosciences, Shizuoka University, Shizuoka 422, Japan.

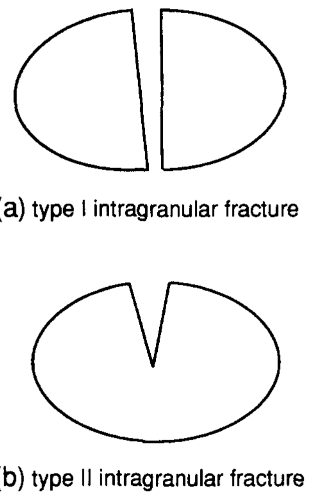

Fig. 1. (a) Type I intragranular fracture. (b) Type II intragranular fracture.

hornblende–biotite granite along Yanazawa Creek (i.e. YG8 in fig. 2b of Michibayashi & Masuda 1993), where the mylonitic foliation strikes from 040° to 020° and dips at approximately 50°NW. The foliation contains a strong stretching lineation trending 010°–030° and plunging between 10° and 30° (Michibayashi & Masuda 1993).

Microstructural studies show that feldspars were plastically deformed at amphibolite facies metamorphic conditions, resulting in dynamic recrystallization along grain boundaries and myrmekite replacement from rim to core in K-feldspar porphyroclasts (Michibayashi & Masuda 1993). Mylonitic fabrics such as S–C fabrics (Berthé *et al.* 1979) and asymmetric strain shadows (Simpson and Schmid 1983) also are well developed within this mylonite, indicating a regional sinistral strike-slip or top-to-the-south sense of shear (cf. Takagi 1986, Michibayashi & Masuda 1993, Yamamoto 1994).

Michibayashi & Masuda (1993) have shown that progressive retrogression led to strain localization during shearing, such that only a narrow zone (width: ca 400 m) along the margins of the plutons was further deformed during later stages of mylonitization. Furthermore, this narrow zone appears to have developed a steady-state grain size (i.e. ca 40 μm; cf. Twiss 1977, Etheridge & Wilkie 1979) in dynamically recrystallized quartz aggregates (Michibayashi 1993). The granitic mylonite was sampled from this narrow zone. Therefore, intragranular fractures discussed in this paper formed at low-T conditions, probably during the latest stage of mylonitization (cf. Michibayashi & Masuda 1993).

INTRAGRANULAR FRACTURES

Although fractures locally affect amphiboles, they predominantly occur in feldspar and hence only the latter are examined in detail. The fractures are intragranular (see Atkinson 1987 for terminology) and can be morphologically subdivided into two sub-types: type I, cutting from one side of a grain to the other (Fig. 1a), and type II, lying within the grain (Fig. 1b). Type I intragranular fractures are by far the more common.

Fractures in K-feldspar

K-feldspar shows weak undulose extinction due to internal ductile deformation prior to fracturing. In larger porphyroclasts, intragranular fractures tend to transect each grain close to the centre, and their walls show local syntaxial K-feldspar overgrowth (Fig. 2a). Segments of fractured porphyroclasts are pulled apart and/or displaced in the fine-grained matrix and the quartz infill has been strongly recrystallized into fine grains (Fig. 2a). The fracture surfaces are not always parallel to one another. This suggests that these segments have been rotated. Also, a deviation from a true extension fracture origin would account for the non-parallelism of the adjacent fracture surfaces (Geoff Lloyd, written communication 1994).

Frequently, intragranular fractures follow along (001) cleavages (Fig. 2a). Twin boundaries have also locally parted and contain quartz infill. Their surfaces are very sharp and few syntaxial overgrowth rims form. Extinction under crossed polars of the porphyroclast shows no conspicuous variation across these cleavage-parallel fractures. These features show that fracture along the cleavage (types I, II and III) was the mechanism largely responsible for intragranular fracturing (Lloyd and Knipe 1992).

Although K-feldspar porphyroclasts are commonly enclosed by myrmekite rims, the fractures generally do not cut through these rims even where fragmented porphyroclasts have been pulled apart over some distance (Fig. 2b). Locally, several cleavage-parallel fractures occur in a single grain. The gaps are slightly wider near the core, but usually terminate towards the rim. This suggests that the fractures are penny-shaped.

Locally, fluorite forms together with quartz in the gaps (Fig. 2b), suggesting that hydrothermal alteration of biotite and/or amphibole along the mylonitic foliation may have occurred (M. Rubenach, personal communication 1992), as biotite and amphibole are commonly altered to secondary minerals such as chlorite. None the less, the existence of fluorite as well as the massive quartz infills in the gaps indicates that the separation of the segments occurred simultaneously with the (dissolution–)precipitation process during the mylonitization (Lloyd & Knipe 1992, Hippertt 1993).

Fractures in plagioclase

Porphyroclastic feldspar is strongly controlled by its crystallography, tending to show semi-rectangular shapes (Fig. 3a). Otherwise, they are rather similar to an ellipsoid. The intragranular fractures in plagioclase tend to occur near the centre of the grain and frequently follow along the (001) cleavage (Fig. 3b). This indicates that fracturing of plagioclase may also be controlled by the cleavage (types I, II and III; e.g. Lloyd and Knipe 1992), although this is not a universal relationship, as illustrated in Fig. 3(a).

The fracture space is commonly filled with quartz that has been locally dynamically recrystallized. Syntaxial

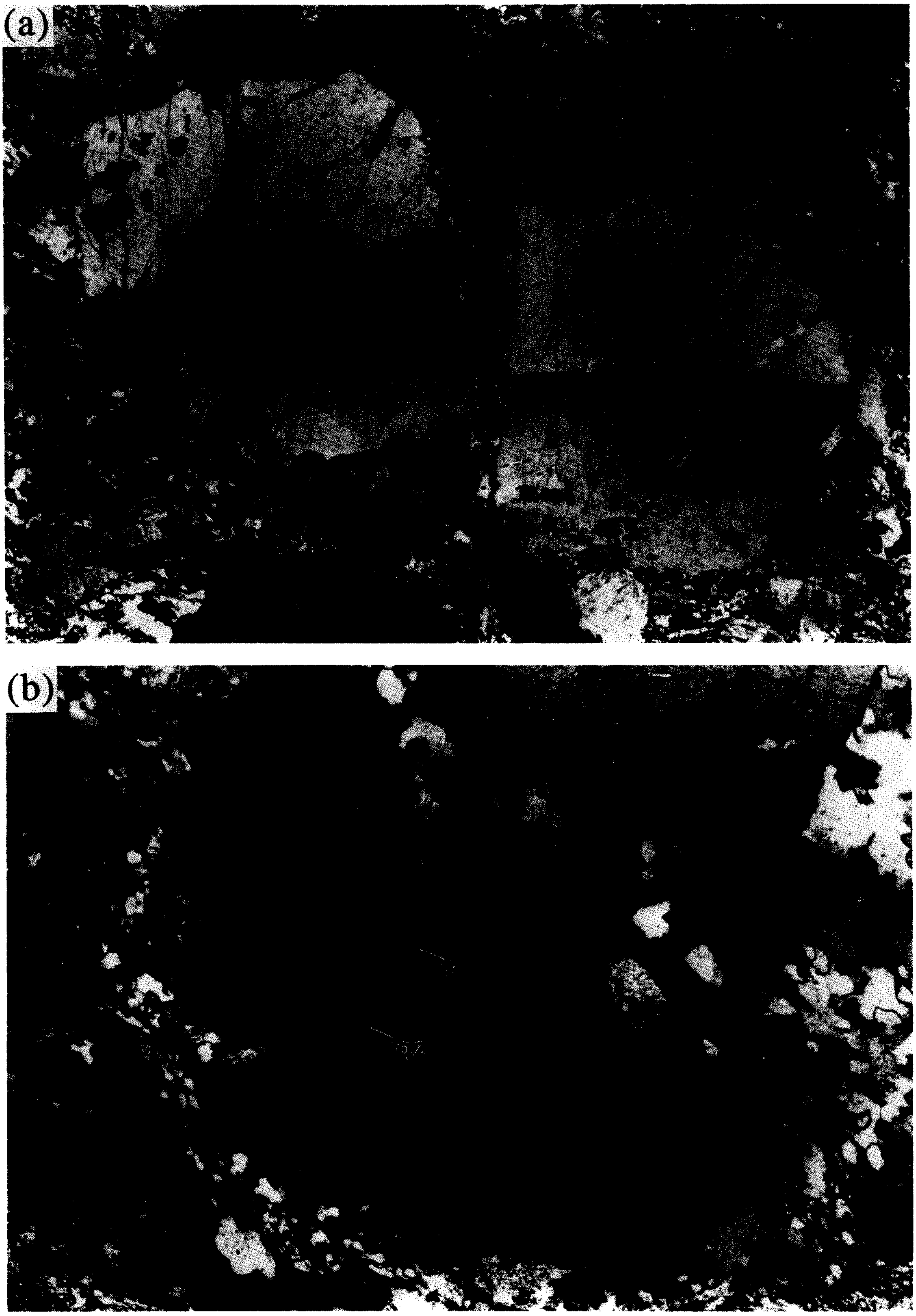

Fig. 2. (a) Fractures in an 'augen' K-feldspar porphyroclast. The fracture at the centre of this grain contains dynamically recrystallized quartz infill. A number of the cleavage-parallel fractures are present plus a fracture along a twin boundary. Crossed polars. Width of base, 16 mm. (b) The intragranular fracture in a K-feldspar porphyroclast occurs near the middle of the grain. This grain is partly surrounded by myrmekite. The gaps are filled with quartz (qz) and fluorite (F). Crossed polars. Width of base 2.25 mm.

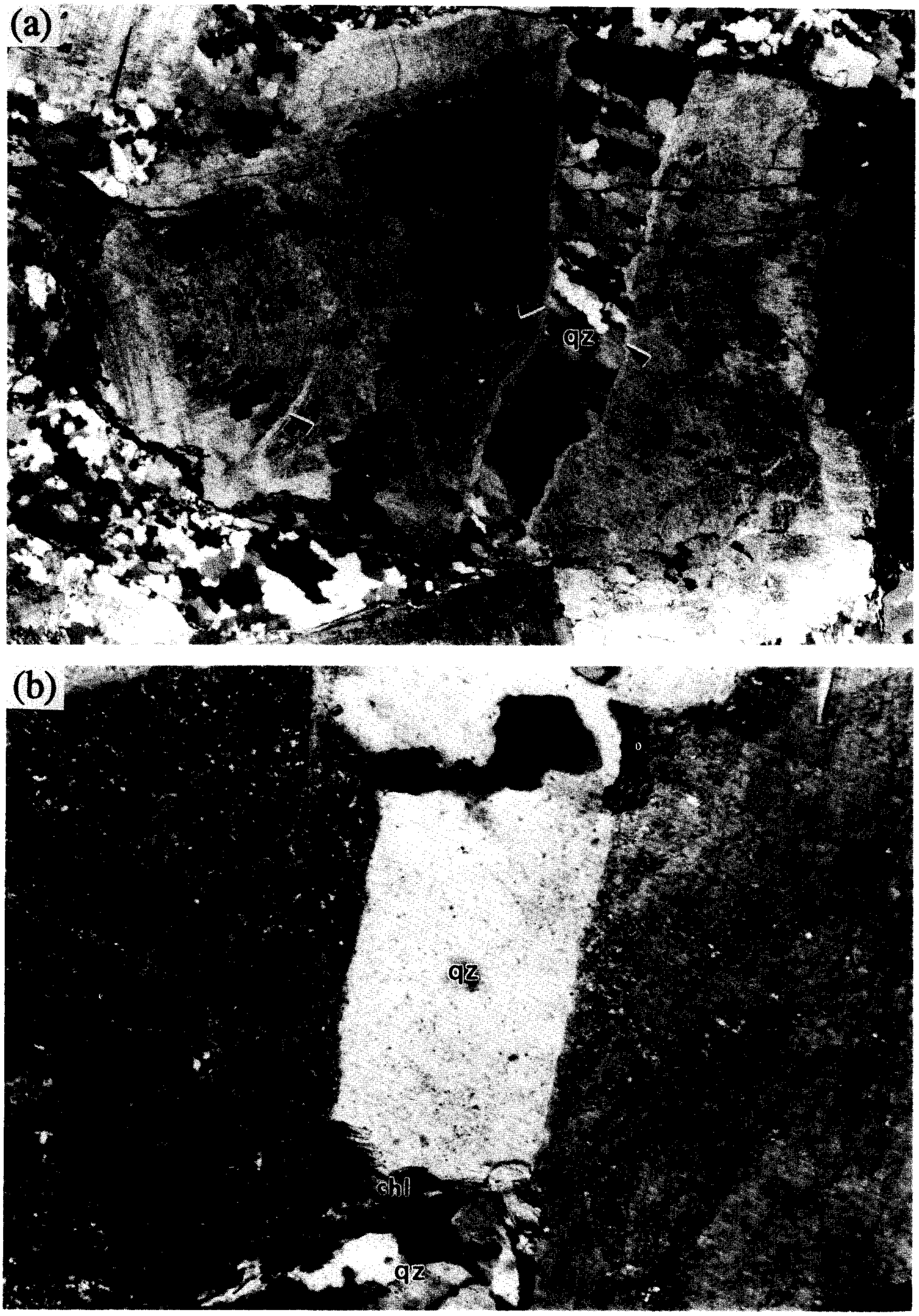

Fig. 3. (a) Intragranular fracture through a plagioclase porphyroclast. The quartz infill (qz) has been dynamically recrystallized to some extent. Syntaxial growth of plagioclase occurs along the walls (arrows). One small fracture is almost completely sealed by syntaxial growth of plagioclase (arrow on left). Width of base 7 mm. (b) Extensional cleavage-parallel fracture in a plagioclase porphyroclast. The gap is bounded by a chlorite folia (chl) and is filled with a single quartz crystal. Width of base 0.75 mm.

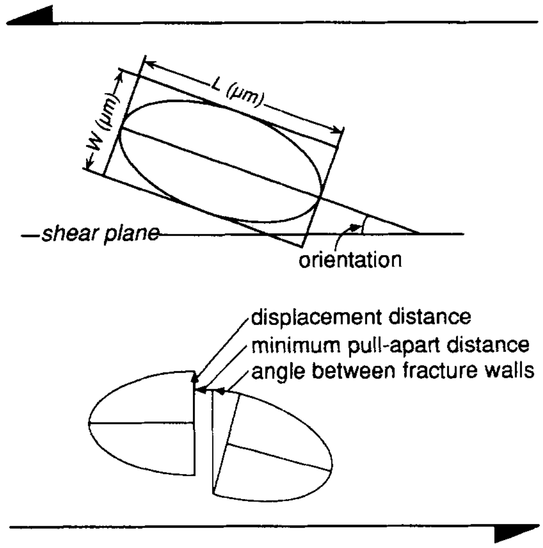

Fig. 4. Schematic diagram to illustrate parameters for a statistical analysis. The clockwise orientation of the long axis with respect to the shear plane is regarded as negative in this paper.

growth of plagioclase occurs on the fracture walls and almost completely seals minor intragranular fractures. Quartz infill is commonly bounded by chlorite foliae, allowing distinction of recrystallized quartz infill from the matrix. Although Bailey *et al.* (1994) suggested that the chlorite foliae around porphyroclasts results from dissolution of the porphyroclast, this is not demonstrable in this mylonite.

Type II intragranular fractures are more common in plagioclase than in K-feldspar. They taper from the grain boundary towards the core, resulting in a *v*-shaped gape (Hippertt 1993) filled by quartz that is only partly recrystallized, or contains a single crystal. This suggests that the fractures initiated at grain boundaries and propagated inwards. Alternatively, they could be half-penny shaped cracks (Geoff Lloyd, written communication 1994).

METHODS TO QUANTIFY INTRAGRANULAR FRACTURES

Figure 4 illustrates parameters used to study development of the intragranular fractures within this mylonite. Thin sections were made in a plane parallel to the mylonitic lineation and perpendicular to the mylonitic foliation. Measurements were made using a microscope with a micrometric ocular. Where intragranular fractures occur in feldspar, separation components between fragments that occur during fracturing were also measured (Fig. 4). The size of an individual grain (d) was determined by:

$$d = \sqrt{LW}, \quad (1)$$

where L is the length of the grain and W is the width perpendicular to L (Fig. 4; e.g. Masuda 1982). The shapes of individual grains can be approximated by ellipses with an aspect ratio (R) that was determined by:

$$R = \frac{L}{W}. \quad (2)$$

The feldspar porphyroclasts in this mylonite were divided into two categories: unbroken grains and broken grains. Unbroken grains are those that have not been fractured, or that contain only type II intragranular fractures terminating within the grain. Broken grains are those that can be restored from two fragments. Although the broken grains do not exist as single grains, their reconstruction is necessary to determine how intragranular fracturing occurred in feldspar.

Fragments resulting from fracturing in broken grains should be classified as unbroken grains, since they are considered to be stable in that stage of mylonitization. Some feldspar grains were fractured progressively during the mylonitization, and older segments were split again. In this case, I counted the older segments as broken grains (cf. Masuda *et al.* 1989).

Where an original broken grain was fractured successively in the same direction, the lengths were always measured in the one direction, even if the fracturing of one grain into two segments caused its length in this direction to become shorter than its width. Thus, the aspect ratio of the segments can be *less than one* (i.e. $W > L$). This procedure is necessary to calculate the aspect ratio of the original grain (Ferguson 1981, 1987).

RESULTS

Grain size

The grain size distribution is log-normal (Fig. 5a), and the average grain size is 760 μm (log d = 2.88). The proportion of fractured grains increases remarkably as the grain size increases (Fig. 5b). Few feldspar grains smaller than ca 320 μm (i.e. log d = 2.5) have fractured during the mylonitization (Fig. 5b). The mean size of the broken grains alone is 1270 μm (log d = 3.1), which is distinctly coarser than that of the unbroken grains (i.e. 690 μm; log d = 2.83).

Grain shape (aspect ratio)

The distribution (Fig. 6a) shows that most feldspar grains have aspect ratios less than three, with an average of 1.78. The proportion of fractured grains rises slightly as the aspect ratio increases to four (Fig. 6b). No fractures occurred within grains with aspect ratios greater than four (Fig. 6b), but this may not be statistically significant because of the small number of grains in this range. The mean aspect of the broken grains alone is 1.91, which is larger than that of the unbroken grains (i.e. 1.76).

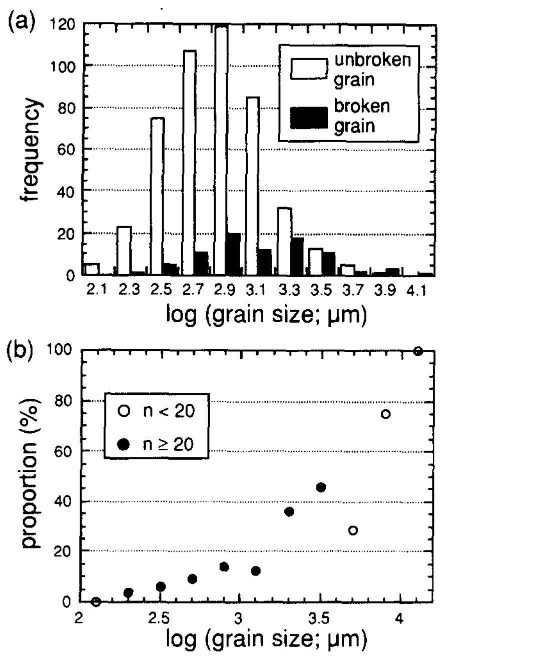

Fig. 5. (a) Frequency of unbroken and broken grains vs logarithmic grain size. The average grain size is 690 μm for unbroken grains and 1270 μm for broken grains, respectively, with a total average of 760 μm. (b) Proportion of broken grains in the grain population with respect to logarithmic grain size. Solid circles show the proportions for more than 20 grains, whereas open circles indicate those for less than 20 grains.

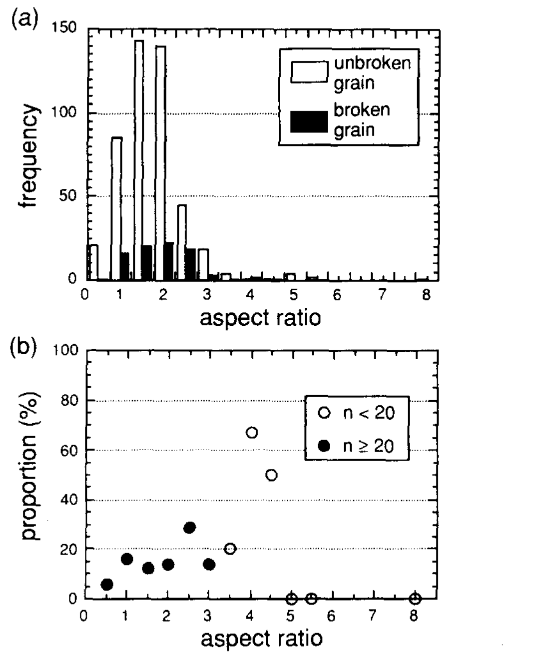

Fig. 6. (a) Frequency of unbroken and broken grains vs aspect ratio. The average aspect ratio is 1.76 for unbroken grains and 1.91 for broken grains, respectively, with a total average of total grains at 1.78. (b) The proportion of broken grains to total grains with respect to aspect ratio. Solid circles show the proportions for more than 20 grains, whereas open circles indicate those for less than 20 grains.

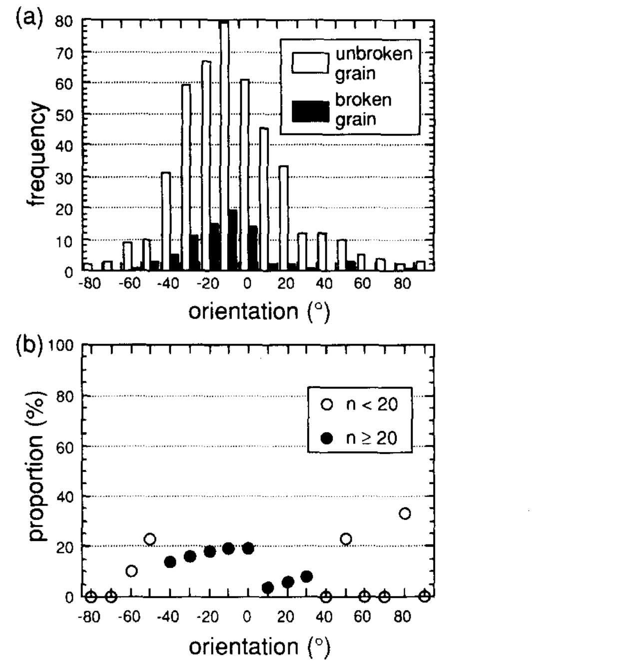

Fig. 7. (a) Frequency of unbroken and broken grains vs orientations of the long axis with respect to the shear plane. The average orientation is −6.9° for unbroken grains and −11.8° for broken grains, respectively, with a total average of −7.6°. (b) The proportion of broken grains in the grain pollution with respect to orientations of the long axis. Solid circles show the proportions for more than 20 grains, whereas open circles indicate those for less than 20 grains.

Shape-preferred orientation

The long axes (lengths) of feldspar grains are strongly oriented at negative angles with respect to the shear plane (Fig. 7a). The mean orientation of whole grains is −7.6° and 80% of the feldspar grains are preferentially oriented between −40° and 20° (Fig. 7a). The proportion of grains that are fractured increases from 10% in grains at −70° to −60° orientation to 20% at −10° to −0° and decreases abruptly to less than 10% at positive angles (Fig. 7b). The mean orientation of broken grains alone is −11.8°, which is more oblique to the shear plane than that of the unbroken grains (i.e. −6.9°).

DISCUSSION

Interpretation of the statistical data

Grain abundance increases and the proportion of the broken grains markedly decreases as grain size decreases (Fig. 5). This indicates that the fractures have preferentially developed in coarser grains during the mylonitization. However, the statistical data show that the grain shape and its preferred orientation also have some effects on intragranular fracturing (Figs. 6 and 7). Therefore, we need to compare these two parameters with the grain size.

The relationship between grain size and aspect ratio for unbroken grains is shown in Fig. 8(a), whereas that for broken grains and their final segments is presented in Fig. 8(b). In order to trace a sequence of fractures in

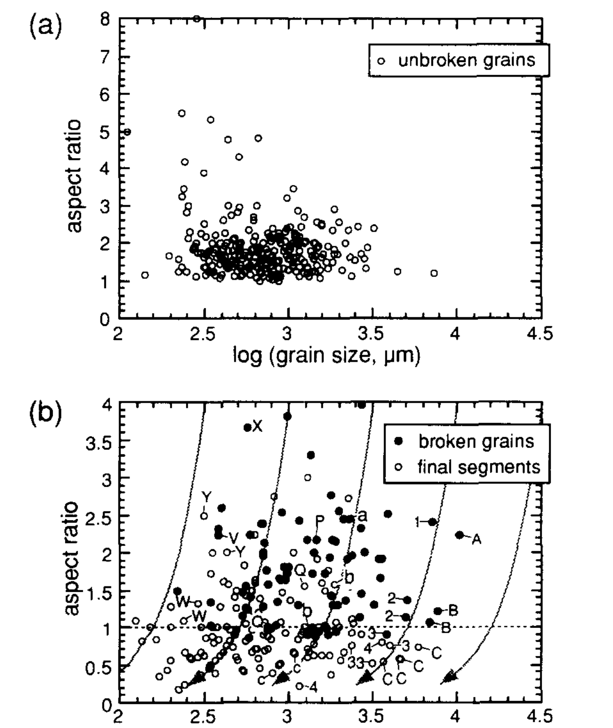

Fig. 8. Grain size (logarithmic scale) vs aspect ratio, (a) for unbroken grains; (b) for broken grains and their final segments. Each curved dashed line shows a constant width regardless of grain size. See the text for details.

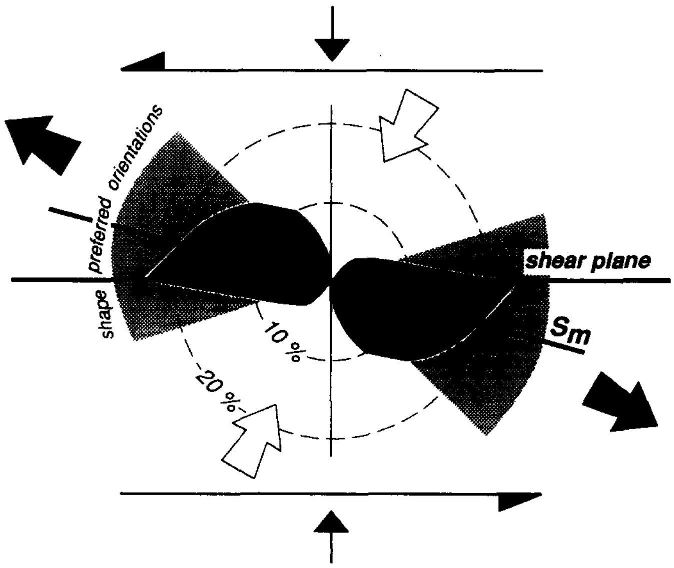

Fig. 9. Rose diagram showing proportions of broken grains with respect to the kinematic frame during the mylonitization. Open arrows indicate the compression field, solid arrows show the extension field. The shape-preferred orientations of feldspars in this mylonite are also marked in this diagram. See text for discussion.

originally coarse grains, Fig. 8(b) presents a series of curves where each one follows a single width for different grain sizes. Most fractures tend to occur perpendicular to the length of a grain, so that the width of grains changes only a little after fracturing. Thus, if a grain has a rectangular shape, the plots of its fractured segments exactly follow a single curve in Fig. 8(b) (see also Fig. 10). In contrast, if a grain shape is irregular, its segments depart from this curve. The fracture sequence of six original grains is traced in Fig. 8(b). Each sequence is labelled A → B → C and 1 → 2 → 3, etc.

Two originally coarse grains (labelled A and 1, respectively) have been repeatedly fractured (labelled B, C and 2, 3, 4, respectively) until the aspect ratios of their segments became less than one (Fig. 8b). Similarly, few fractures occurred in feldspars with an aspect ratio less than one, although the grains are still large enough to be fractured (compare Fig. 8b with Fig. 5). This suggests that grain size was not the only factor controlling the development of fractures.

Notice that where aspect ratios of segments became less than one, their 'true' longest axes were actually placed *perpendicular* to the extension direction. This is because most of the broken grains were originally arrayed sub-parallel to the extension direction (Fig. 7). Figure 7 shows that fractures are mainly extensional rather than shear fractures (Boullier, written communication 1994). Therefore, the development of intragranular fractures in these grains resulted in a change of shape-preferred orientation, by which fractured segments would be prevented from further fracturing (Fig. 9). As a consequence, the probability of fracturing would become remarkably small in these grains, although their grain size is still large enough to allow fracturing. This is principally due to the effect of shape preferred orientation control on fracturing in conjunction with the grain shape.

Possibility of a stable grain size for fracturing

Few fractures occurred within the smaller grains (Fig. 8b), although their aspect ratios are higher than those of larger grains. This suggests that the fracture process becomes less effective with grain size reduction. Moreover, the average grain size of all feldspar grains changed only a little before and after fracturing (776–691 μm; Fig. 5). This may indicate that a diameter of ca 700 μm represents an equilibrium size for feldspar grains at that stage of mylonitization. It would be interesting now to measure feldspars in other samples showing different states of finite strain to verify if this equilibrium grain size varies across the low-*T* shear zone.

A similar tendency to that described above has been reported for a complete shear zone: Boullier (1980) has shown for the Pan-African mobile belt of Iforas that the average grain size of feldspars decreased markedly as a result of fracturing, becoming stable with increasing strain. This clearly indicates that grain size reduction due to fracturing became less effective during progressive shearing. Consequently, the development of intragranular fracturing could not occur within grains with sizes below a critical value.

With respect to the average aspect ratio in feldspar, the grain shape of the feldspar porphyroclasts appears to be relatively stable during mylonitization. Boullier (1980, fig. 11) showed that the average aspect ratio of feldspars was fairly constant, in a range between 1.3 and 1.7 from the margin to the centre of the shear zone, even though their grain size decreased. Takagi (1984) showed a similar tendency for the average aspect ratio of thirty plagioclase porphyroclasts in each sample across the Kashio Shear Zone in the vicinity of Takato–Ichinose, Japan. These aspect ratios slightly decreased, from 1.8 to 1.5, across the shear zone (fig. 10 in Takagi, 1984). The data presented in this study show that aspect ratios are dominantly in the range between 1.0 and 2.0 with an average of 1.56 (Fig. 6). Thus, the aspect ratio of porphyroclasts in mylonite may be generally regarded to be approximately constant at around 1.5.

Grain size reduction due to fracture–rotation–reshaping processes: a model

In Fig. 8(b), sequences of fracturing in grains were traced in which fracturing has ceased where aspect ratios became less than one. However, I suggest that, since in these sequences grain size is still larger than the maximum stable size of 700 μm, two possible processes could enable feldspars to reduce their grain size further during the mylonitization.

In Fig. 10, aspect ratios are justified with respect to the extension field in the range between −45° and 20°. If the long axis of a grain is oriented in this range, the aspect ratio is defined as L/W. However, if the long axis is not oriented in this range, the aspect ratio is determined as W/L, where its width is judged to be the length. This results in an aspect ratio smaller than one (Fig. 10a). In this way, when a grain is rotated towards the extension field, the justified aspect ratio in Fig. 10(a) changes. For instance, if the justified aspect ratio changed from 1/2 to 2 as a result of rotation into the extension field, the point moves vertically from D to D* in Fig. 10(a) (see also Fig. 10c). This means that the final fragment, D, is shifted from one fracture sequence to the start of the other fracture sequence, at D* (Fig. 10a). This could result in D* having a higher probability of being fractured. This fracture–rotation process could continue until the broken grains eventually reach relatively stable grain sizes (the shaded area in Fig. 10a). It may be interesting to note that if a coarse grain underwent the cyclic fracture–rotation process and a fracture occurred at the mid-point of a grain (Fig. 10b), the aspect ratio of the broken grains will always be between one and two, independent of the original aspect ratio.

Alternatively, the justified aspect ratio can change by re-shaping of the grain (Fig. 10d). Unlike rigid minerals such as tourmaline and garnet, felspars deform plastically or brittley depending on temperature (Tullis & Yund 1985, 1987). Therefore, fracture walls could be subsequently deformed or modified during progressive shearing. If the broken grain (2) in Fig. 10(a) were internally deformed to lose parts of its volume due to recrystallization, dissolution, or minor fracturing along grain boundaries, it may shift gradually from (2) to (3) (see also Fig. 10d). This fracture re-shaping process is quite suitable for grain size reduction in feldspar. The re-shaped grain, (3), could again be fractured to reduce its grain size unless it reached a relatively stable size (the shaded area in Fig. 10a).

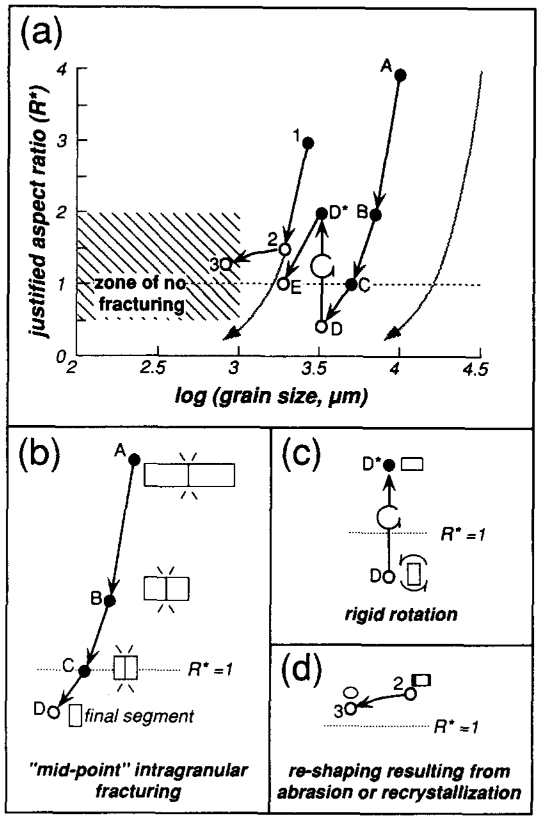

Fig. 10. (a) Schematic diagram of grain size vs aspect ratio showing processes of the grain size reduction in feldspar. A justified aspect ratio is determined by the length of a grain with respect to the extension field. The labels in the diagram (e.g. A and 1, etc.) correspond with rectangular grains in (b) and (c). The zone of no intragranular fracturing is marked as cross-hatched area, where the microfracturing in feldspar could cease during the mylonitization. (b) Grain size reduction due to 'mid-point' intragranular fracturing. A sequence of microfracturing is indicated as A–B–C–D. (c) Justified aspect ratio changed from ½ to 2 as a result of rigid rotation into the extension field, so that the grain D moved vertically to D*. (d) Grain size reduction due to a reshaping process. The sequence (2)–(3) is connected by reshaping the grain of (2) as a result of abrasion, recrystallization or dissolution. The broken grain labelled (2) reaches the zone of no fracturing by the reshaping process. See text for discussion.

Natural deformations can be more complicated so that fracturing, rotation and re-shaping may occur simultaneously, resulting in a cyclic grain size reduction. However, although fracturing is the most effective way to reduce grain size, further grain size reduction would result only from re-shaping processes if a feldspar grain has reached the stable grain size for fracturing. Moreover, if this re-shaping process ceases, the grain remains stable.

Deformation mechanism of microfracturing

Tensile intragranular fractures occurred near the centre of grains, breaking them into two halves. The fractured segments were subsequently separated (e.g. Figs. 2 and 3). These features are compatible with the fibre-loading mechanism in brittle minerals (see also Boullier 1980, White *et al.* 1980, Lloyd *et al.* 1982). It should be noted that the kinematic frame for the mechanism is essentially considered to be coaxial (Masuda *et al.* 1989, Ji and Zhao 1993). This assumption seems to counteract the fact that the kinematic frame for mylonite is generally considered to be non-coaxial. However, since intragranular fractures dominantly occurred in the extension direction (Fig. 9), the development of intragranular fracturing in this mylonite could occur analogously by a similar kinematic frame to fibre-loading in a coaxial direction.

CONCLUSIONS

Grain size was apparently the most important parameter for fracturing in feldspar from the Kashio shear zone, since a critical grain size (ca 700 μm) developed during the mylonitization below which little fracturing occurred. This means that grain size reduction in feldspar due to fracturing is predominantly in coarse porphyroclasts, and that the fracturing ceases with grain size reduction. The grain shape (aspect ratio) and the shape-preferred orientation also affect the development of fracturing. The fragments that lie sub-perpendicular to the extension direction may resist fracturing regardless of grain size, unless they rotate towards the extension field or their shape is modified to be elongated parallel to the extension direction. It should be stressed that the measurements have been performed on one sample and that the 700 μm value is only valid for the stage of mylonitization experienced by this sample.

Acknowledgements—J. Hippertt, W. Huang and T. Masuda are acknowledged for their stimulating discussions; T. Bell and R. Ross for improving the English. J. Tullis, S. Ji, G. Lloyd, A.-M. Boullier, L. Pryer and J. Hippertt are gratefully acknowledged for their detailed comments and criticisms of an earlier version of this manuscript. This paper was financially supported by an Overseas Postgraduate Research Scholarship and a James Cook University Postgraduate Research Scholarship.

REFERENCES

Atkinson, B. K. 1982. Subcritical crack-propagation in rocks: theory, experimental results and applications. *J. Struct. Geol.* **4**, 41–56.

Atkinson, B. K. 1984. Subcritical crack growth in geological materials. *J. geophys. Res.* **89**, 4077–4114.

Atkinson, B. K. 1987. *Fracture Mechanics of Rock*. Academic Press, London.

Bailey, C. M., Simpson, C. & De Paor, D. G. 1994. Volume loss and tectonic flattening strain in granitic mylonites from the Blue Ridge province, central Appalachians. *J. Struct. Geol.* **16**, 1403–1416.

Berthé, D., Choukroune, P. & Jégouzo, P. 1979. Orthogneiss, mylonite and non coaxial deformation of granites: the example of the South Armorican Shear Zone. *J. Struct. Geol.* **1**, 31–42.

Boullier, A. M. 1980. A preliminary study on the behaviour of brittle minerals in a ductile matrix: example of zircons and feldspars. *J. Struct. Geol.* **2**, 211–217.

Cox, H. L. 1952. The elasticity and strength of paper and other fibrous materials. *Br. J. appl. Phys.* **3**, 72–79.

Etheridge, M. A. & Wilkie, J. C. 1979. Grainsize reduction, grain boundary sliding and the flow strength of mylonites. *Tectonophysics* **78**, 475–508.

Ferguson, C. C. 1981. A strain reversal method for estimating extension from fragmented rigid inclusions. *Tectonophysics* **79**, T43–T52.

Ferguson, C. C. 1987. Fracture and separation histories of stretched belemnites and other rigid-brittle inclusions in tectonites. *Tectonophysics* **139**, 255–273.

FitzGerald, J. D. & Stunitz, H. 1993. Deformation of granitoids at low metamorphic grade. I: reactions and grain size reduction. *Tectonophysics* **221**, 269–297.

Hanmer, S. K. 1981. Segregation bands in plagioclase: non-dilational quartz veins formed by strain enhanced diffusion. *Tectonophysics*, **79**, T53–T61.

Hanmer, S. K. 1990. Natural rotated inclusions in non-ideal shear. *Tectonophysics* **149**, 245–255.

Hara, I., Shoji, K., Sakurai, Y., Yokoyama, S. & Hide, K. 1980. Origin of the Median Tectonic Line and its initial shape. *Mem. geol. Soc. Japan* **18**, 27–49.

Hara, I., Yamada, T., Yokoyama, S., Arita, M. & Hiraga, Y. 1977. Study on the southern marginal shear belt of the Ryoke metamorphic terrain—initial movement picture of the Median Tectonic Line. *Chikyu Kagaku* **31**, 204–207 (in Japanese with English abstract).

Hippertt, J. F. M. 1993. "V"-pull-apart microstructures: a new shear sense indicator. *J. Struct. Geol.* **15**, 1393–1403.

Ji, S. & Zhao, P. 1993. Location of tensile fracture within rigid-brittle inclusions in a ductile flowing matrix. *Tectonophysics* **220**, 23–31.

Kano, K. 1978. Stratigraphy and structure of the Ryoke metamorphic rocks in Aichi Prefecture, Central Japan. *J. geol. Soc. Japan* **84**, 445–458 (in Japanese with English abstract).

Lloyd, G. E., Ferguson, C. C. & Reading, K. 1982. A stress-transfer model for the development of extension fracture boudinage. *J. Struct. Geol.* **4**, 355–372.

Lloyd, G. E. & Knipe, R. J. 1992. Deformation mechanisms accommodating faulting of quartzite under upper crustal conditions. *J. Struct. Geol.* **14**, 127–143.

Masuda, J. 1982. A microstructural sequence of quartz schists in central Shikoku, southwest Japan. *Tectonophysics* **83**, 329–345.

Masuda, T. Michibayashi, K. & Ohta, H. 1995. Shape preferred orientation of rigid particles in a viscous matrix: re-evaluation to determine kinematic parameters of ductile deformation. *J. Struct. Geol.* **17**, 115–129.

Masuda, T., Shibutani, T., Igarashi, T. & Kuriyama, M. 1989. Microboudin structure of piedmontite in quartz schists: a proposal for a new indicator of relative palaeodifferential stress. *Tectonophysics* **163**, 169–180.

Michibayashi, K. 1993. Syntectonic development of a strain independent steady state grain size during mylonitization. *Tectonophysics* **222**, 151–164.

Michibayashi, K. & Masuda, T. 1993. Shearing during progressive retrogression in granitoids: an abrupt grainsize reduction of quartz at the plastic–brittle transition for feldspar. *J. Struct. Geol.* **15**, 1421–1432.

O'Hara, K. 1990. Brittle–plastic deformation in mylonites: an example from the Meadow Fork thrust, western Blue Ridge province, southern Appalachians. *Geol. Soc. Am. Bull.* **102**, 1706–1713.

Ohtomo, Y. 1993. Origin of the Median Tectonic Line. *J. Sci. Hiroshima Univ. Ser. C* **9**, 611–669.

Passchier, C. W. 1987. Stable positions of rigid objects in non-coaxial flow—a study in vorticity analysis. *J. Struct. Geol.* **9**, 679–690.

Passchier, C. W. & Simpson, C. 1986. Porphyroclast systems as kinematic indicators. *J. Struct. Geol.* **8**, 831–843.

Prior, D. J. 1993. Sub-critical fracture and associated retrogression of garnet during mylonitic deformation. *Contr. Miner. Petrol* **113**, 545–556.

Ryoke Research Group. 1972. The mutual relations of the granitic rocks of the Ryoke metamorphic belt in Central Japan. *Chikyu Kagaku* **26**, 205–216 (in Japanese with English abstract).

Simpson, C. & Schmid, S. M. 1983. An evaluation of criteria to deduce the sense of movement in sheared rocks. *Bull. geol. Soc. Am.* **94**, 1281–1288.

Takagi, H. 1984. Mylonitic rocks along the Median Tectonic Line in Takato–Ichinose area, Nagano Prefecture. *J. geol. Soc. Japan* **90**, 81–100 (in Japanese with English abstract).

Takagi, H. 1986. Implications of mylonitic microstructures for the geotectonic evolution of the Median Tectonic Line, central Japan. *J. Struct. Geol.* **8**, 3–14.

Takagi, H. & Ito, M. 1988. The use of asymmetric pressure shadows in mylonites to determine the sense of shear. *J. Struct. Geol.* **10**, 347–360.

Tullis, J. & Yund, R. A. 1985. Dynamic recrystallization of feldspar: a mechanism for ductile shear zone formation. *Geology* **13**, 238–241.

Tullis, J. & Yund, R. A. 1987. Transition from cataclastic flow to dislocation creep of feldspar: Mechanisms and microstructures. *Geology* **15**, 606–609.

Twiss, R. J. 1977. Theory and applicability of a recrystallized grain size paleopiezometer. *Pure & App. Geophys.* **115**, 227–244.

White, J. C. & White, S. H. 1983. Semi-brittle deformation within the Alpine fault zone, New Zealand. *J. Struct. Geol.* **5**, 579–589.

White, S. H., Burrows, S. E., Carreras, J., Shaw, N. D. & Humphreys, F. J. 1980. On mylonites in ductile shear zones. *J. Struct., Geol.* **2**, 175–187.

Yamamoto, H. 1994. Kinematics of mylonitic rocks along the Median Tectonic Line, Akaishi Range, central Japan. *J. Struct. Geol.* **16**, 61–70.